Analysis of robustness of steel frames against progressive collapse

Analysis of robustness of steel frames against progressive collapse

Liu-Lian Li[1,2], Guo-Qiang Li[1,3,*], Bin-hui Jiang[1] and Yong-Lu[4]

[1]*College of Civil Engineering, Tongji University, Shanghai 200092, PR China*
[2]*China State Construction Technical Center，Beijing 101300，PR China*
[3]*State Key Laboratory for Disaster Reduction in Civil Engineering, Tongji University, Shanghai 200092, PR China*
[4] *Institute for Infrastructure and Environment, School of Engineering, University of Edinburgh, Edinburgh EH9 3JL, UK*

Abstract: A finite element (FE) modelling study on the progressive collapse of steel frames under a sudden column removal scenario is presented. The FE models were developed with refined shell elements using the general purpose FE software package ABAQUS. The FE models were first validated by comparing the predicted responses with the measured results from an experimental study on the progressive collapse of three steel frame specimens. A new bearing capacity-based index was introduced to quantify the robustness of the steel frames. The robustness index takes into account the dynamic effects and the plastic internal force redistribution. By incorporating the experimental results and the numerical simulations, the dynamic amplification factor in the progressive collapse of the steel frames was assessed. The validated FE models were further applied to identify the collapse modes of planar steel frames and evaluate the influences of a range of mechanical and geometrical parameters on the progressive collapse and the robustness. The results showed that, for a column-instability induced progressive collapse mode, the influences of the damping is larger than the influences of the strain rate of material on the robustness. However, for the connection-failure induced progressive collapse mode, the influences of the strain rate is larger than the damping. The type of the steel frame (e.g. weak-beam strong-column or vice versa) and the location of the column removal were both found to play an important role in influencing the critical load and the robustness of steel frames.

Keywords: steel frame; progressive collapse; bearing capacity; robustness; critical load; collapse modes.

[*]Corresponding author, Tel: +86-21-65982975, Email: gqli@tongji.edu.cn

1. Introduction

Prevention of progressive collapse and improving the robustness of structures in withstanding local failure has become a key area of research in structural engineering ever since the collapse of Ronan Point tower in 1968[1], and research effort further intensified following the collapse of Alfred P. Murrah building in Oklahoma (1995)[2] and the collapse of the World Trade Center Towers in 2001[3]. The key characteristic of progressive collapse is the distinct disproportion between the triggering limited failure and the resulting widespread collapse; structures which are prone to progressive collapse are generally considered as having insufficient robustness[4].

Robustness is a broad term used in a variety of contexts. In control theory, for instance, robustness is defined as a measure of insensitivity of a system to effects that are not considered in the design[5]. Similarly, a statistical technique is said to be robust if it is insensitive to small deviations in the assumptions[5]. In the context of progressive collapse, robustness is a desirable property of structure which helps to mitigate the structural susceptibility to progressive collapse or disproportionate collapse[6, 7].

Robustness of a structure is strongly related to the internal structural characteristics such as redundancy, ductility and the behaviour of connections and it also depends upon the type and location of local damage [8]. To assess the robustness of a building structure against progressive collapse following an element loss, a quantitative measure of robustness would be desirable [6], such that a single value may be used to express how and to what extent the building structure is influenced by local failures [9]. Over the last decades, a number of studies on the quantification of structural robustness or related characteristics have been reported. Below, a brief overview is presented and the detailed review of research development on structural robustness can be found in Li et.al [10].

In principle, the studies on the quantitative assessment of structural robustness may be

divided into two categories, namely, using structural attributes-based measures and using structural behaviour-based measures. Agarwal et.al [11-14] used a graph model and the topological relation of a structure to develop a vulnerability theory to assess the robustness of trusses structure. GSA2003 [15] adopted the Demand-Capacity Ratios (DCR) of connections to quantify the robustness of a structure. Huo et.al [16] defined a ductility measure for connections as the rate of ultimate rotation capacity under an impact and to the rotation at which the catenary action began to form. Such a ductility rate was suggested to assess the robustness of a structure. Starossek and Haberland [6, 9] introduced a robustness measure based on the static stiffness of a structure.

The robustness measures based on the structural behaviour are often derived from the response of a structure to an assumed initial local failure [9]. Based on the bearing capacity, Huang and Li [17], Gao and Liu [18] proposed the importance coefficients of components to evaluate the structural robustness quantitatively. Feng and Moses [19], Frangopol and Curley [20] adopted structural redundancy to quantify the robustness of structure. Biondini et.al[21] proposed a robustness index associated with the displacements of the structure under different states. Based on the quantification of the damage progression resulting from initial damage, the damage-based robustness measure was proposed by Starossek and Haberland [6, 9, 22]. By comparing the energy released during an initial failure and the energy required for failure to progress, several energy-based robustness measures have been proposed by different researchers [6, 9, 22-25]. By dividing the risk into direct risk associated with initial local damage and indirect risk associated with subsequent system failure, Baker el.al[5] introduced a probabilistic risk assessment-based robustness measure. Frangopol et.al [20, 26] proposed a reliability-based robustness measures by considering the failure probability of damaged structure and the failure probability of intact structure. Liao et.al[27] employed the structural reliability and redundancy concept and proposed a ratio of spectral acceleration

of steel frame to evaluate the robustness quantitatively.

Despite of a variety of approaches to the formulation for the robustness measures, however, there is still a lack of a uniform theory for the structural robustness assessment and a general methodology for the quantification of the progressive collapse resistance of real complex structures [28]. Most of the existing robustness indexes involve arbitrary definitions and have not fully considered the effects of structural characteristics, local damage and dynamic effects on the robustness. Moreover, most of the quantifications for structural robustness are based on the elastic analysis without considering the plastic internal force redistribution of structures.

This paper presents a study on the robustness of steel frames under a sudden column removal scenario based on nonlinear finite element analysis of the progressive collapse process of the structure. Using the bearing capacity, a new method for the quantification of robustness is proposed for steel frames. The quantitative robustness index takes into account the dynamic effects and the plastic internal force redistribution within a frame structure. In order to evaluate the critical load of the damaged frame upon collapse, the possible progressive collapse modes of the steel frame following the sudden removal of a column are identified. With the aid of the validated finite element models, the influences of other pertinent parameters, namely the material strain rate, damping, the relative size of the beam and column sections, the load ratio (defined as the ratio of the load imposed on the frame to the elastic limit load of the frame), as well as the location of the removed column on the progressive collapse and robustness are analysed and discussed.

2. Overview of the experimental investigation

Prior to the present numerical study, an experimental investigation was conducted into the progressive collapse of steel frames under a column removal scenario. The details of the

experiment have been presented in a separate paper [29]. Herein a brief summary of the test programme and key findings are summarised for the sake of numerical model verification and comparison.

The progressive collapse tests were conducted on three two-storey, four-bay planar steel frames. The test setup and steel frame are schematically shown in Fig 1. The properties of the test frames are listed in Table 1. In the experiment, the sudden removal of middle column at the first storey was simulated by a special removal mechanism column along with a pendulum hammer. The column removal process is shown in Fig. 2. Firstly, the "column" to be removed was assembled to the steel frame specimen prior to the loading and the suspending baskets were set up to simulate gravity loads. Then, the pendulum hammer was pulled to the designated position and subsequently released suddenly and knocked the removable column, as shown in Fig. 2a. The brittle glass rod which held the removable column in place was broken by impact of the pendulum hammer, and this led the removable column to become a mechanism and lost the load carrying function, thus resembling a sudden removal of the column (Fig.2b). The out-of-plane movements of the test frames were restrained by an out-of-plane supporting setup. Weights simulating the desired gravity loads were attached to the test frame through suspended baskets. Details of the experimental process can be found in [29].

Table1. Summary of the properties of test steel frames

Specimen	Beam section	Column section	Story height		Span length
			h_1	h_2	l
	mm	mm	mm	mm	mm
FRAME1	Middle bay: H54×50×4×4 Side bay: H80×50×3×4	H100×100×6×8	1227	1054	2100
FRAME2	H54×50×4×4	H54×50×4×4	1227	1054	2054

FRAME3	H54×50×4×4	H100×100×6×8	1227	1054	2100

The experiment results indicate that the time taken for the removable column to be removed was around 0.02 sec, which was well within $1/10^{th}$ of the dominant natural frequency (about 0.5s). After the sudden removal of the middle column, one steel frame failed as the columns adjacent to the removed column failed in bending and compression, whereas for the other two steel frames, significant local buckling was developed at the bottom flange of beams. Fig. 3 shows the final global damage of the FRAME2 and Fig. 4 shows the final local damage of the steel frames at the beam ends.

3. Finite-element analysis and validation

3.1 Finite-element model

The finite element models of the experimental steel frames were established with the refined shell elements using ABAQUS. The finite-element analyses were conducted by using the explicit dynamic solver to facilitate the calculations of the high-speed dynamic responses involving complex nonlinear processes such as contact, large deformation and fracture. Similar to the experimental configuration, out-of-plane displacements of each beam were constrained at the midspan. The bases of the column at the ground storey were modelled as fully fixed. Fig. 5a shows the finite element model of specimen FRAME1.

To cater to the large deformation analysis, four-node shell elements with reduced integration (S4R) were used to simulate the beams and columns of the steel frames. As generally understood, the mesh size is an important factor that affects both the accuracy and efficiency of the explicit dynamic analysis. Smaller mesh size tends to produce more accurate analysis results. However, smaller mesh size increases the computing cost and this is particularly true in an explicit analysis as the stable time increment is inversely related to

the mesh size. For this reason, a mesh convergence and efficiency study was carried out, and by comparing the analysis results of different mesh sizes, the optimal mesh sizes were identified. In the vicinity of the beam-to-column connection, the beams and columns were meshed with an element size of about 12 mm. In regions away from the connection zones, the beams and columns were meshed with an element size of 25 mm, as shown in Fig. 5b.

3.2 Material properties

In order to simulate the dynamic behaviour of the steel frame specimens induced by a fast column removal with large deformations more realistically, the material model based on the true stress - strain relationship has to be employed in the finite element analyses. The true stress - strain relationship can be derived from material property data from tensile steel coupon tests which are usually in the form of engineering stress and strain. Using the data of engineering stress, σ_{Eng}, and strain, $\varepsilon_{\mathrm{Eng}}$, the true stress, σ, and true strain, ε, can be obtained by the following equations:

$$\varepsilon = \ln\left(1+\varepsilon_{Eng}\right); \qquad \sigma = \sigma_{Eng}\left(1+\varepsilon_{Eng}\right) \tag{1}$$

Before stress hardening, the stress-strain relationship of steel in the finite-element analyses can be described with a bi-linear model. The Ramberg-Osgood equation, which can capture the nonlinear behaviour of the steel, is used to model stress-strain behaviour of the steel in the stress hardening stage. The power-law hardening model of the Ramberg-Osgood equation can be written as [30, 31]:

$$\varepsilon = \varepsilon_e + \varepsilon_p = \frac{\sigma}{E} + \left(\frac{\sigma}{\sigma_0}\right)^m \tag{2}$$

where ε_e is the elastic strain, ε_p is the plastic strain, E is Young's modulus, m is the hardening exponent for the “plastic” (nonlinear) term and σ_0 is the reference stress value. According to the data of the true stress and strain which were obtained from engineering

stress and strain through coupon tensile tests, the parameters m and σ_0 can be calculated by [31]:

$$\sigma_0 = \left(\frac{\sum_{i=1}^{N} \sigma_i^m}{\sum_{i=1}^{N} \varepsilon_{pi}} \right)^{\frac{1}{m}} \quad (3)$$

$$m = \frac{\sum_{i=1}^{N} \ln \varepsilon_{pi}}{\sum_{i=1}^{N} \ln \frac{\sigma_i}{\sigma_0}} \quad (4)$$

where σ_i is the true stress and ε_{pi} is the true plastic strain. The parameters m and σ_0 are listed in Table 2. To give a further validation of the above stress-strain model, a comparison is made between the true stress-strain curves obtained from the coupon tests of the H54×50×4×4 section webs and those obtained from Eq. 2, as shown in Fig. 6. It is seen that the steel stress-strain model is in good agreement with the test results.

Tab. 2 Material property model parameters for steel stress-strain model

		σ_y/MPa	m	σ_0/MPa
H54x50x4x4	web	417.0	8.84	821.97
(Q345)	flange	394.5	8.40	730.47
H80x50x3x4	web	326.2	5.96	748.42
(Q235)	flange	318.3	6.77	684.25
H100x100x6x8	web	409.8	5.26	943.83
(Q345)	flange	386.2	6.59	849.27

For ductile materials like steel, damage and fracture initiation can be described by plastic deformation. The damage evolution law, which is characterized by the progressive degradation of the material stiffness in a linear form for steel[32], can be specified in terms of the equivalent plastic displacement which is dependent on the characteristic length of the element and equivalent plastic strain of material [33]. Ductile fracture would occur after the

material underwent extensive necking and plastic deformation in the necked region. Fracture in steel may be modelled using element erosion, in which elements are deleted from the model when a specified value of the effective plastic strain is attained [34, 35]. In the present finite element model, the value of erosion strain was determined by the equivalent plastic strain corresponding to steel fracture based on the tensile tests of the steel coupons, and this will be further explained later in Section 5.2.

Under blast and impact loadings, the progressive collapse of structures triggered by a sudden loss of a vertical support member is a dynamic process involving high strain rates [36]. Considering that steel materials are generally sensitive to the strain rates, it is appropriate to take into account the strain rate effects on the compressive and tensile yield strengths of steel in the progressive collapse analysis. In the present finite element analysis, the Cowper-Symond model is employed:

$$\frac{\sigma_{\mathrm{yd}}}{\sigma_y} = 1 + \left(\frac{\dot{\varepsilon}}{C}\right)^{\frac{1}{P}} \qquad (5)$$

where σ_y is the static yield stress, σ_{yd} is the dynamic yield stress, $\dot{\varepsilon}$ is the strain rate and C and P are the material parameters. The Cowper–Symonds model is a phenomenological material equation, thus the parameters have to be determined from experimental observations[37]. According to the experimental results reported in [38] and suggestions in the research literature [39, 40], the material parameters C and P were taken to be 40.4 /s and 5 respectively for steel material considered herein.

The damping effect is modelled using the Rayleigh damping model[33]. To define Rayleigh damping, the damping factors α and β, which depict the mass proportional damping and stiffness proportional damping, respectively, need to be specified. Considering the fact that for in a progressive collapse process the structure behaviour is dominated by lower frequency components, the mass proportional damping was used to represent the

damping of the structures in the present study. The damping ratio was adopted as 5% for all the three test steel frames.

3.3 Simulation of column removal

The removal of the middle column at the first storey of the steel frame specimens was simulated with the following procedure.

The undamaged frame was firstly statically analysed under the applied loads, and the axial force incurred in the middle column at the first storey of the frame, F_{max}, was determined.

The frame is then analysed without the removable column, and instead, its effect is represented by the axial force as obtained from the above initial static analysis. This process is simulated by slowly applying the axial load until F_{max} is reached, as illustrated in Fig. 7 and 8. The duration for F to reach F_{max} is set as Δt_1 = 7s, which is greater than 10 times of the fundamental vertical vibration period of the frame without the middle column. As such the process of applying F on the structural behaviour can be regarded as quasi-static [41], thus preserving a static equilibrium state. The reaction force at F_{max} is maintained for a short period (Δt_2 = 0.05s in Fig.8) for further stabilisation. From there, the column removal can be easily simulated by a rapid reduction of the F force until it reaches zero, as also shown in Fig. 8. In the present analysis, the duration for the removal of the axial force F is set as Δt_3 = 0.02s.

In order to ensure that the dynamic characteristics of the finite-element model is consistent with the steel frame specimens, an equivalent density of the beams is obtained for the FE model taking into account the loading set-up parts, including the struts and the steel rollers that were mounted on the beams to present the out-of-plane movement.

3.4 Comparison with experimental measurements

Table 3 lists the fundamental vertical vibration frequencies of the steel frame specimens obtained from the experiments and from the FEM analysis when the middle bottom column was removed. It is seen that the numerical simulation results are in reasonable agreement with experimental results, indicating that the finite-element models are able to capture the dynamic characteristics of the test specimens.

Tab. 3 Fundamental vertical vibration frequencies of frame specimens.

Frequency/Hz	FRAME1	FRAME2	FRAME3
FE model	2.06	1.85	2.01
Experiment	2.34	1.75	2.31

As a representation of the primary response of the steel frames under the sudden column removal scenario, the vertical deflections of the steel frames at the location of the removed column obtained from the FE analysis and experimental measurements are compared in Fig.9. Good agreement is observed between the experimental and analytical deflection results.

To give a further validation of the finite-element model, the strains and internal forces at representative locations are also compared. Fig. 10 show the comparison of the strain time histories at the beam sections B_1 and B_3 between the analytical results and experimental results for FRAME1 and FRAME2 after the middle column removal. Table 4 lists the internal forces at beam sections of B_1 in both FRAME1 and FRAME2 as obtained from experimental measurements and from the FEM analysis. All these comparisons also exhibit a good agreement; the maximum differences are generally within 10% between the FE analysis and experimental results.

Table 4 Internal forces at beam section B_1 of frame specimens

Specimen	Measured		Analyzed with FEM	
	Axial force (kN)	Moment (kN.m)	Axial force (kN)	Moment (kN.m)

FRAME1	52.5	4.46	53.8	3.95
FRAME2	22.8	5.22	22.9	5.42

From the above comparisons, it can be observed that the finite-element models can reliably predict the behaviour and dynamic response of the steel frames in the event of a sudden column loss. The FE models can therefore be employed for further evaluation of the detailed responses and for parametric calculations.

4. Bearing capacity-based robustness index

As mentioned in the Introduction, in the present study the characteristic of a structure against progressive collapse in the event of a local failure is referred to as "robustness". Such structural robustness is directly related to the ability of the structure to redistribute the loads and remain stable following the local failure such as a column removal [42]. According to this definition, a bearing capacity-based robustness measure for steel frames can be obtained by comparing the load imposed on the original intact structure (Fig.11a), and the residual load capacity of the damaged structure in which a prescribed column is removed (Fig.11b). The bearing capacity-based robustness index can thus be written as:

$$I_{rob} = \frac{(q_{2m} - \gamma q_{1m})}{q_{2m}} = \frac{(q_{2dm} - q_{1m})}{q_{2dm}} \qquad (6)$$

where q_{1m} is the load carried by on the intact structure, which can be represented by the load imposed on the two middle bays adjacent to the removed column, while load carried by the side bays is denoted as q_{1s} as shown in the figure. The maximum values of q_{1m} and q_{1s} can be considered as the elastic limit load of intact structure (Fig.11a). q_{2m} is the static critical load of the middle bays for the damaged structure until failure (Fig.11b) and q_{2s} is the corresponding static critical load of the side bays for the damaged structure. γ is a dynamic amplification factor, and q_{2dm} is the dynamic critical load of the middle bays for the damaged structure until failure, which may be obtained by $q_{2dm} = q_{2m}/\gamma$.

In order to obtain the critical load of the damaged structure to failure, it is necessary to identify first the possible progressive collapse modes of a steel frame following a column removal. Two most important progressive collapse modes have been classified according to the extent of the progressive collapse associated with a particular failure condition [43]. The first progressive collapse mode is classified as the contained progressive collapse mode (CCM) [43] (Fig.12a), in which the progressive collapse is largely limited to just the damaged bays. The contained progressive collapse is initiated by the fracture of beam or the failure of the beam-to-column connection[44]. The second progressive collapse mode is identified as a propagating progressive collapse mode (PCM) [43] (Fig.12b), in which progressive collapse propagates to adjacent bays. In steel frames, the propagating progressive collapse is primarily induced by the buckling of the columns surrounding the removed columns[45]. Therefore, the propagating progressive collapse mode is also referred to as a loss-of-stability induced progressive collapse mode[45].

We can see directly from Eq. (6) that the proposed robustness index can explicitly account for the dynamic effects and considers the plastic internal force redistribution. If $I_{rob} \leq 0$, the critical load of the damaged structure is smaller than the load imposed on the intact structure, thus the progressive collapse may occur and the frame is lacking necessary robustness. On the other hand, if $I_{rob} > 0$, the frame is generally robustness and may not collapse. A hypothetical upper limit for I_{rob} is equal to 1, and values close to 1 means the critical load of the damaged frame is considerably larger than the initial load carried by the frame. Between 0 to 1, the larger the I_{rob} value, the better the robustness of the frame.

5. Dynamic effects and Progressive Collapse modes

5.1 Dynamic effects

The removal of a column will cause a steel frame to enter into a new deformation phase.

The dynamic effect due to a fast column removal will cause large deformation of the steel frame than that due to a slow column removal in which the dynamic effects may be ignored. A dynamic amplification factor, γ, due to the column removal on steel frame can be defined as the ratio of the static force to the dynamic force that will cause an equal deformation response [46].

Using the finite element models validated above and considering material nonlinearity and geometrical nonlinearity, a push-down analysis is carried out for the three steel frames under consideration. Fig. 13 shows the applied load, P_{1m}, versus static vertical displacement at the removed column location for the three frames. It can be seen that, for FRAME1, the static load corresponding to a vertical displacement equal to the experimental vertical displacement of 0.252m is P_{1m} = 4.42kN (or q_{1m} = 1.26kN). From the experiment, the applied load that caused the above displacement was 3.3 kN. Thus, the dynamic amplification factor can be obtained as γ_1 = 4.42/3.3 = 1.34. For FRAME2 and FRAME3, the dynamic amplification factors are found to be γ_2 = 4.23/3.85 = 1.10 and γ_3 = 4.57/3.85 = 1.19, respectively. It should be noted that the dynamic amplification factor γ are much smaller than the conventional value 2.0, and this is attributable to the energy dissipation due to the plastic deformations developed in the frame specimens.

Fig. 14 presents the deformations of FRAME1 obtained by a direct dynamic analysis and by a static analysis considering the dynamic amplification factor, respectively. It is seen that results from the static analysis including the dynamic amplification agrees well with the dynamic analysis result. This indicates that a static analysis considering an appropriate dynamic amplification factor is an efficient approach to a progressive collapse analysis.

5.2 Progressive collapse modes

To expose the progressive collapse modes of the steel frame specimens following a sudden

removal of the middle column at the ground storey, dynamic analyses of column removal have been carried out with the applied loads increased to a level by which signs of progressive collapse can be clearly observed.

In the process of progressive collapse large deformation will develop and in local areas fracture of the material can occur. As mentioned in Section 3.2, in the FE model herein fracture is modelled by element erosion. The erosion criterion is set in accordance with plastic equivalent strain, and the erosion limit for the steel and welds are estimated from the plastic equivalent strain according to the coupon test results. When the respective limit is reached in any element, the element is deleted, thus resembling a physical fracture process in an explicit manner. For FRAME1, the loads on the middle two bays and on the side bays are increased to P_{1m} = 9.45kN (q_{1m} = 2.70kN) and P_{1s} = 4.89kN (q_{1s} = 1.40kN), respectively, after preliminary trial analyses. The results from the dynamic analysis with the removal of the middle column at the ground storey indicated the formation of plastic zones with extensive plastic deformation near the column bases, with substantial beam deflections along the line of the removed column. When the vertical deflection of the beams reached 836mm, the rotation of beam-to-column connection reached 0.398 rad, and fracture occurred at the top beam flanges and it propagated into the web; at the same time, significant local buckling appeared in the bottom flange near the connections, as shown in Fig. 15. The first floor beams in the middle bays were found to have developed an axial tension force of 90 kN, which is 0.38 times of the axial yielding force of the section. Finally, the frame collapse occurred due to the buckling of the columns surrounding the removed column as shown in Fig. 16.

Similar dynamic analyses were also performed for FRAME2 and FRAME3, and the results including the deformation patterns and the axial forces in the first floor beams at the critical state of collapse are shown in Fig. 16 and Tables 5, respectively. It can be seen that,

under the condition that the beam-to-column connections are sufficiently ductile, the progressive collapse of a steel frame will be governed by the buckling of the columns surrounding the removed column at the first storey.

Table 5 Critical loads inducing progressive collapse of steel frame specimens under the middle column removal

Specimen	critical load P_{1m} (kN) at middle bay	critical load P_{1s} (kN) at side bay	axial force (kN)	Progressive Collapse mode
FRAME1	9.45	4.89	90 ($0.38N_y$*)	Column instability
FRAME2	4.62	2.52	37 ($0.16N_y$)	Column instability
FRAME3	10.85	5.98	113 ($0.48N_y$)	Column instability

*Note: N_y – axial yielding capacity of the beam.

6. Parametric studies

In order to investigate the factors affecting the robustness and the behavior of general steel frames after a column loss, five parameters were chosen for parametric studies. These parameters included the strain rate effect of material, damping, sizes of beam and column sections, load ratio (the load imposed on the frame/the elastic limit load of the frame), and the location of the removed column.

6.1 Effects of material strain-rate sensitivity and damping

As a representation, the influences of the material strain-rate sensitivity and the damping were examined by analysing FRAME1 using the validated FE model. The middle bay load (q_{1m}) and the side bay load (q_{1s}) were assumed to be 2.30kN and 1.19kN, respectively. It should be noted that if the strain rate and damping effects were ignored, the respective critical loads of q_{2dm} and q_{2ds} in this FRAME1 were 2.40kN and 1.24kN, respectively and the progressive collapse occurred due to the buckling of the ground story columns surrounding the removed column.

The influences of considering the material strain rate effect, as per the default definition in Abaqus for steel material (in accordance to Cowper-Symond model), and a 5% damping on the deflection time histories at the removal location are depicted in Fig 17. When neither of the strain rate or damping was considered, the permanent deflection was 1220mm and the rotation of beam-to-column connection reached 0.581 rad in the frame bays where the column was removed. However, when both the strain rate effect and a 5% damping were considered, the permanent deflection reduced to 809mm and the rotation of beam-to-column connection reduced to 0.385 rad, respectively. Therefore, the strain rate and damping effects contributed to a significant reduction in the maximum permanent deflection and the rotation of beam-to-column connection of the frame bays where the column was removed, by 33.69% and 33.73%, respectively. If the damping was considered only, the maximum permanent deflection was 925mm (24.18% reduction) and the maximum rotation of beam-to-column connection was 0.440 rad (24.26% reduction). If the strain rate effect was considered only, however, the permanent deflection was 1188mm (2.62% reduction) and the rotation of beam-to-column connection was 0.566 rad (2.58% reduction). In fact, the strain rates were observed to vary in different parts of the frame and at different times, and the maximum strain rate was up to about 32 s^{-1} for FRAME1 during the process of collapse in all four studied cases herein. Overall, in the case of a column-instability induced collapse mode, the influences of the damping appear to be larger than the influences of the strain rate effect of the material.

To further examine the influence of varying the damping ratio on the progressive collapse resistance, FRAME1 was analysed under a nominal imposed load q_{1m} of middle bay at the elastic limit of 1.60 kN and the side bay imposed load q_{1s} of 0.82kN as obtained from the intact frame. The standard strain-rate effect of the material was included in the analysis. Table 6 lists the critical load q_{2dm} and q_{2ds}, the robustness I_{rob} and the collapse

mode of damaged FRAME1 for different damping ratio ξ. It is seen that, for the column-instability induced progressive collapse mode, the critical load and robustness increase with increasing the damping ratio. The I_{rob} values indicate the frame is robustness under all the different damping effects and is not prone to collapse after the removal of the middle column.

Table 6 List of q_{2dm}, q_{2ds}, I_{rob} and collapse mode for FRAME1 under different damping ratios

The damping ratio ξ	Critical load q_{2dm}（kN）	Critical load q_{2ds}（kN）	Robustness I_{rob}	Collapse mode
0.000	2.449	1.262	0.347	Column instability
0.020	2.551	1.314	0.370	Column instability
0.035	2.651	1.366	0.397	Column instability
0.050	2.703	1.392	0.410	Column instability

Since all three frames considered thus far had a column-instability induced collapse mode, a further finite element model, FRAME4, was developed to represent a progressive collapse mode induced by the beam-to-column connection failure. This frame was subsequently studies to observe the influences of the strain rate effect of the material and the damping (with a fixed damping ratio of 0.05). Table 7 summarises the dimensions of FRAME4. In order to simulate the fracture of fully welded connections, the weld material, which possessed a relatively small fracture strain, was set to cover a 10mm length from the beam end. The stress-strain constitutive relationships of Q235 steel and the weld material were obtained according to the coupon test results[32, 47]. The column removal period was set almost instantaneous. All the other settings of model parameters are the same as those of FRAME1. An overview of the finite element model of FRAME4 is shown in Fig. 18.

Table 7 The geometric dimensions of the FRAME4 and FRAME5

FE Models	The size of the beam section	The size of the column section	The story height		The span length l
			h_1	h_2	
	mm	mm	mm	mm	mm
FRAME4	H100×100×4.5×6 (Q235)	H100×100×6×8 (Q235)	1000	900	1600
FRAME5	H100×100×4.5×6	H100×100×6×8	1250	1100	2100

The analysis of FRAME4 was performed assuming a middle bay load, P_{1m}, of 35kN and the side bay load, P_{1s}, of 15kN. If the strain rate and damping were both ignored, the critical load P_{2dm} and P_{2ds} of FRAME4 were 36.1 kN and 15.2 kN, respectively and the progressive collapse occurred due to the failure of connections, as illustrated in Fig.19.

A comparison of the deflection time histories of FRAME4 following the removal of the first floor centre column without and with the consideration of the effects of the strain rate and the damping are shown in Fig 20. When neither the strain rate nor the damping was considered, the permanent deflection was 268mm and the rotation of beam-to-column connection was 0.168 rad in the frame bays where the column was removed. When both the strain rate and the damping were considered, the permanent static deflection was reduced to 212mm and the rotation of beam-to-column connection was reduced to 0.133 rad. For the damping-only case, the permanent static deflection was 260mm and the rotation of beam-to-column connection was 0.163 rad. However, for the strain rate-only case, the permanent static deflection was 219mm and the rotation of the beam-to-column connection was 0.137 rad. It is noted that the maximum strain rate reached about 10 s^{-1} for FRAME4 during the process of collapse for four studied cases. Overall, for the connection-failure induced progressive collapse mode, the influences of the strain rate of the material is larger than the influences of the damping.

Considering an imposed load P_{1m} on the middle bay at the intact elastic limit load of

43 kN and the side bay at P_{1s} 18.17kN, FRAME4 was also analysed to examine the influences of varying the damping ratio while keeping the material strain rate effect. Table 8 lists the critical load P_{2dm} and P_{2ds}, the robustness I_{rob} and the collapse mode of damaged FRAME4 for different damping ratios. It is seen that, for the connection-failure induced progressive collapse mode, the critical load and robustness increase with increasing the damping ratio in a similar trend as in column-stability induced progressive collapse cases.

Tab. 8 P_{2dm}, P_{2ds}, I_{rob} and collapse mode for different damping ratio ξ

The damping ratio ξ	Critical load P_{2dm}（kN）	Critical load P_{2ds}（kN）	Robustness I_{rob}	Collapse mode
0.00	47.03	19.88	0.085	Connection failure
0.02	48.52	20.52	0.113	Connection failure
0.035	49.04	20.74	0.122	Connection failure
0.05	49.53	20.94	0.140	Connection failure

6.2 The effects of the sizes of beam and column section

A further finite element model, FRAME5, was also developed to represent a common steel frame of a standard design, to examine the influences of the sizes of beam and column sections. The dimensions of the frame are also listed in Table 7. The material model of Q345 is identical to that of middle bay beams of FRAME1. All the other settings of the model parameters are same as those of FRAME1.

The critical load q_{2dm} and q_{2ds} for FRAME5 were found to be 6.51 kN and 3.35kN, respectively, and the progressive collapse occurred due to the buckling of the ground story columns surrounding the removed column, as shown in Fig. 21.

In order to study the effect of the sizes of beam and column sections on the critical load and the robustness of steel frames, a series of variant frame cases from FRAME5 were created with a varying size of the beam sections. In particular, a beam section size of

H100×100×3.2×4.5 was chosen to represent a strong column-weak beam frame and another size of H100×100×6×8 was chosen to represent a strong beam-weak column frame, respectively. Table 9 summarise the results for different frames, including the elastic limit load of q_{1e} for the intact state, the critical load q_{2dm} and q_{2ds}, the robustness I_{rob} (the imposed load q_{1m} equals to q_{1e}) and the collapse mode of damaged frame. It is seen that, for the strong beam-weak column frame, the critical load and robustness is larger. However, for the strong column-weak beam frame, the critical load and robustness is smaller.

Table 9 Summary of q_{1e}, q_{2dm}, q_{2ds}, I_{rob} and collapse mode for different variants of FRAME5

Type of steel frame	q_{1e} （kN）	q_{2dm} （kN）	q_{2ds} （kN）	I_{rob}	Collapse modes
Common frame (FRAME5)	6.51	6.51	3.35	0.00	Column instability
Strong column - weak beam frame	5.31	5.12	2.83	-0.04	Column instability
Strong beam-weak column frame	5.00	8.49	4.38	0.06	Column instability

6.3 The effects of the load ratio

Based on the FRAME5 model, the effect of the load ratio, which is defined as a ratio of the load imposed on the intact frame (q_{1m}) to the elastic limit load of the intact frame (q_{1e}), on the final deflection and robustness of steel frame is studied. For the FMRAE5 model, the critical load q_{2dm} and q_{2ds} were found to be 6.51kN and 3.35kN, respectively and the collapse mode was the column-instability induced collapse mode, as shown in Fig. 21.

Four different load ratios (q_{1m}/q_{1e}) were chosen for a parametric analysis, namely 0.25, 0.50, 0.75 and 1. Table 10 lists the final deflection, the robustness I_{rob} and the collapse mode of the damaged frames for the above different load ratios. It is seen that the final deflection increases but the robustness decrease with increasing the load ratio.

Tab. 10 List of Δ_u, I_{rob} and collapse mode for different load ratios

Load ratio P_{1c}/P_{1e}	Imposed load P_{1c}（kN）	Final deflection Δ_u（mm）	Robustness I_{robd}	Collapse modes
0.25	1.63	17.7	0.75	No collapse
0.50	3.25	80.0	0.50	No collapse
0.75	4.87	361	0.25	No collapse
1	6.51		0	Column-instability induced collapse

6.4 The effects of the location of the removed column

Based on the FRAME5 model, the effect of the location of the removed column on the critical load and robustness of steel frames is studied. For the reference case with the middle column removed as in the original FRAME5, the critical load q_{2dm} and q_{2ds} were 6.51kN and 3.35kN, respectively and the collapse mode was the column-instability induced collapse mode (see Fig. 21).

Table 11 List of q_{2dm}, I_{rob} and collapse mode for different column removal locations

Location of the removed column	Critical load q_{2dm}（kN）	Robustness I_{rob}	Collapse mode
Middle column	6.51	0.00	Column instability
Side-bay, interior column	4.71	-0.38	Column instability
Side column	4.86	-0.25	|Beam-fracture induced collapse

Three different column removal locations were chosen, namely (i) a middle column, (ii) a side-bay interior column, and (iii) a side-bay exterior column (side column). Table 11 lists the critical load q_{2dm}, the robustness I_{rob} and the collapse mode of damaged frame for different removed column models, and the collapse modes are illustrated in Fig. 22. It should be noted that the critical load q_{2dm} on the middle bay is the same as the critical load q_{2ds} on the side bay for the removed column case (ii) and removed column (iii). It is seen that, in

the case of a middle column removal, the critical load and robustness is the largest. On the contrary, in the case of a side-bay interior column removal, the critical load and robustness is the smallest. Following the removal of the middle column or a side-bay interior column, the progressive collapse occurred due to the buckling of the ground story columns. However, the progressive collapse occurred due to the fracture of beam following the removal of the side column.

7. Conclusions

A finite element modelling study has been conducted to investigate the progressive collapse behaviour of steel frames under a column removal scenario. The FE models were first validated against the experiments of three steel frame specimens in terms of the dynamic responses and collapse modes. Based on the load bearing capacities, a new index is proposed to evaluate the robustness of steel frames quantitatively. The robustness and critical loads of steel frames with a range of different geometrical and mechanical parameters were subsequently investigated using the validated finite element models. The following main conclusions can be drawn:

1. The FE models with refined shell elements for steel sections achieved good agreement with the experimental results, thus provided good numerical models for detailed progressive collapse analysis and the evaluation of robustness of steel frame structures subjected to a sudden column loss.
2. For the test steel frames, the dynamic amplification factor γ was found to be in a range of 1.10 to 1.34. For these steel frames, a progressive collapse was deemed to be associated with the buckling of the ground story columns surrounding the removed column.
3. For a column-instability induced progressive collapse mode, the influences of the

damping was found to be larger than the influences of the strain-rate sensitivity of the material. However, for a connection-failure induced progressive collapse mode, the influences of the strain rate of the material was larger than the influences of the damping. In general, the critical load and robustness increases with increasing the damping ratio.

4. The critical load and robustness in a strong beam-weak column frame is larger than in a strong column -weak beam frame.
5. The critical load and robustness is larger in the case of a middle column removal. On the contrary, in the case of a side-bay interior column removal, the critical load and robustness is smaller.

Further research is required to establish a more systematic and quantitative correlation between the robustness of steel frames with different frame design and variation of the material parameters.

Acknowledgments

The study presented in this paper was supported by the National Natural Science Foundation of China through Grant No. 51120185001, which is gratefully acknowledged.

References

[1] Pearson, C. and N. Delatte, Ronan point apartment tower collapse and its effect on building codes. Journal of Performance of Constructed Facilities, 2005. 19(2): p. 172-177.

[2] Corley, W., et al., The Oklahoma City Bombing: Summary and Recommendations for Multihazard Mitigation. Journal of Performance of Constructed Facilities, 1998. 12(3): p. 100-112.

[3] Bažant, Z. and Y. Zhou, Why Did the World Trade Center Collapse?—Simple Analysis. Journal of Engineering Mechanics, 2002. 128(1): p. 2-6.

[4] Starossek, U., Progressive collapse of structures. 2009.

[5] Baker, J.W., M. Schubert, and M.H. Faber, On the assessment of robustness. Structural Safety, 2008. 30(3): p. 253-267.

[6] Starossek, U. and M. Haberland, Approaches to measures of structural robustness. Structure and Infrastructure Engineering, 2011. 7(7): p. 625-631.

[7] Brett, C. and Y. Lu, Assessment of robustness of structures: Current state of research. Frontiers of Structural and Civil Engineering, 2013. 7(4): p. 356-368.

[8] Sørensen, J.D., Framework for robustness assessment of timber structures. Engineering Structures, 2011. 33(11): p. 3087-3092.

[9] Starossek, U. and M. Haberland. Evaluating measures of structural robustness. in Proceedings of the Structures Congress. Reston, ASCE. 2009.

[10] Li Liu-lian, et al., A Review on the Research of Robustness of Civil Structures. Progress in Steel Building Structures, 2015(5): p. 5-17. (in Chinese)

[11] Agarwal, J., D. Blockley, and N. Woodman, Vulnerability of systems. CIVIL ENGINEERING SYSTEMS, 2001. 18(2): p. 141-165.

[12] Blockley, D., et al., Structural vulnerability, reliability and risk. Progress in Structural Engineering and Materials, 2002. 4(2): p. 203-212.

[13] Agarwal, J., D. Blockley, and N. Woodman, Vulnerability of structural systems. Structural Safety, 2003. 25(3): p. 263-286.

[14] Agarwal, J., D. Blockley, and N. Woodman, Vulnerability of 3-dimensional trusses. Structural Safety, 2001. 23(3): p. 203-220.

[15] Administration(GSA), U.S.G.S., Progressive Collapse Analysis and Design Guidelines for

New Federal Office Buildings and Major Modernization Projects. 2003, General Services Administration, Office of Chief Architect.

[16] Huo Jingsi, et al. Analysis of dynamic behavior and ductility of steel moment frame connections. Journal of Civil Architectural & Environmental Engineering, 2012, 34 (Suppl.1) : 149-154. (in Chinese)

[17] Huang Liang and Li Long. A quantification method of structural robustness. Engineering Mechanics, 2012,29(8):213-219.(in Chinese)

[18] Gao Yang and Liu Xila. Importance coefficients of components in evaluation of structure robustness. Journal of Rock Mechanics and Engineering, 2008, 27(12) : 2575-2584. (in Chinese)

[19] Feng, Y. and F. Moses, Optimum design, redundancy and reliability of structural systems. Computers & structures, 1986. 24(2): p. 239-251.

[20] Frangopol, D. and J. Curley, Effects of Damage and Redundancy on Structural Reliability. Journal of Structural Engineering, 1987. 113(7): p. 1533-1549.

[21] Biondini, F., D. Frangopol, and S. Restelli. On Structural Robustness, Redundancy, and Static Indeterminacy. in Structures Congress. 2008.

[22] Starossek, U. and M. Haberland. Measures of structural robustness–requirements and applications. in ASCE SEI Structures Congress 2008. Vancouver, Canada.

[23] Beeby, A., Safety of structures, and a new approach to robustness. Structural Engineer, 1999. 77(4): p. 16-21.

[24] Smith, J.W., Structural robustness analysis and the fast fracture analogy. Structural engineering international, 2006. 16(2): p. 118-123.

[25] Fang Zhaoxin and Li Huiqiang. Safety and robustness of structures from the viewpoint of energy. Journal of Building Structures, 2007, 28(Suppl.1) : 269-273. (in Chinese)

[26] Fu, G. and D.M. Frangopol, Balancing weight, system reliability and redundancy in a multiobjective optimization framework. Structural Safety, 1990. 7(2): p. 165-175.

[27] Liao, K.-W., Y.-K. Wen, and D. Foutch, Evaluation of 3D steel moment frames under earthquake excitations. II: Reliability and redundancy. Journal of structural engineering, 2007. 133(3): p. 471-480.

[28] Lu, D.-G., et al., Robustness assessment for progressive collapse of framed structures using pushdown analysis methods. International Journal of Reliability and Safety, 2012. 6(1-3): p. 15-37.

[29] Li, G.-Q., et al., Experimental study on progressive collapse resistance of steel frames under a sudden column removal scenario. Journal of Constructional Steel Research, 2017. Under Review.

[30] Margetson, J., Tensile stress/strain characterization of non-linear materials. The Journal of Strain Analysis for Engineering Design, 1981. 16(2): p. 107-110.

[31] Su Mingzhou and YuYan, Nonlinear tensile stress-strain curves of structural steel. Journal of Xi'an University of Architecture and Technology (Natural Science Edition), 1999. 31(1): p. 25-28. (in Chinese)

[32] Song Zhensen, Damage cumulation collapse mechanism and design ctriteria of welded steel beam-to-column connection under seismic load [D]. Xi'an: Xi'an University of Architecture and Technology, 2001. (in Chinese)

[33] Corp, D.S.S., ABAQUS 6.11 Analysis Users Manual. Abaqus 6.11 Documentation, 2011.

[34] Sadek, F., et al., Testing and analysis of steel and concrete beam-column assemblies under a column removal scenario. Journal of Structural Engineering, 2011. 137(9): p. 881-892.

[35] Yang, B. and K.H. Tan, Numerical analyses of steel beam–column joints subjected to catenary action. Journal of Constructional Steel Research, 2012. 70: p. 1-11.

[36] Santafe Iribarren, B., et al. Effect of concrete rate dependent behaviour on structural progressive collapse. in Proceedings of the 8th International Conference on Structural Dynamics-EURODYN. 2011.

[37] Hernandez, C., et al., A computational determination of the Cowper–Symonds parameters from a single Taylor test. Applied Mathematical Modelling, 2013. 37(7): p. 4698-4708.

[38] NormanJones, Structural impact. 1997: Cambridge University Press.

[39] Liew, J.Y.R., Survivability of steel frame structures subject to blast and fire. Journal of Constructional Steel Research, 2008. 64(7): p. 854-866.

[40] Al-Thairy, H. and Y. Wang, A numerical study of the behaviour and failure modes of axially compressed steel columns subjected to transverse impact. International Journal of Impact Engineering, 2011. 38(8): p. 732-744.

[41] Zhuang Zhuo., et al, Nonlinear Finite Element Analysis and Examples of ABAQUS. First edition. 2005, Beijing: Science Press. (in Chinese)

[42] Vlassis, A., et al., Progressive collapse of multi-storey buildings due to failed floor impact. Engineering Structures, 2009. 31(7): p. 1522-1534.

[43] Khandelwal, K. and S. El-Tawil, Pushdown resistance as a measure of robustness in progressive collapse analysis. Engineering Structures, 2011. 33(9): p. 2653-2661.

[44] Sideri, J., et al., Ductile progressive collapse mechanisms of steel moment frames, in Safety,

Reliability, Risk and Life-Cycle Performance of Structures and Infrastructures. 2014, CRC Press. p. 5053-5058.

[45] Gerasimidis, S., et al., Loss-of-stability induced progressive collapse modes in 3D steel moment frames. Structure and Infrastructure Engineering, 2015. 11(3): p. 334-344.

[46] Tsai, M.-H. and B.-H. Lin, Dynamic amplification factor for progressive collapse resistance analysis of an RC building. The Structural Design of Tall and Special Buildings, 2009. 18(5): p. 539-557.

[47] Xie Fuzhe, Analysis and assessment and experimental research on progressive collapse of steel frame structure [D]. Nanjing: Southeast University, 2012. (in Chinese)

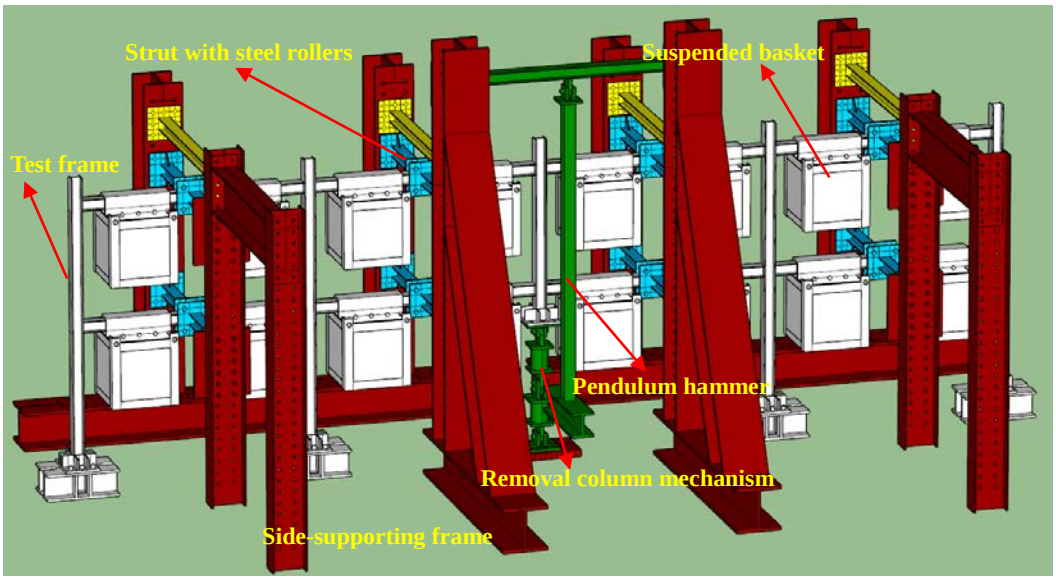

Fig.1 Schematic of test setup and steel frame

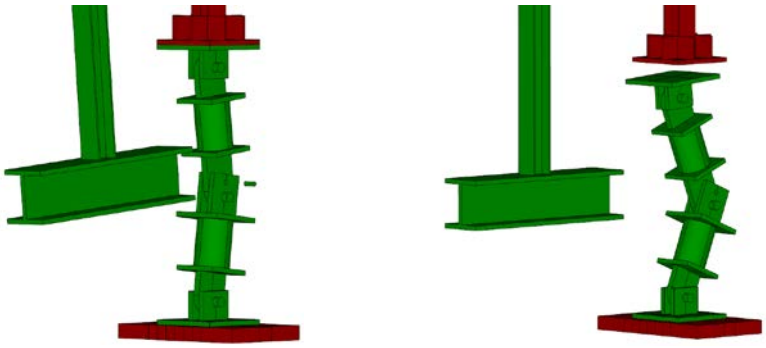

a. Breaking of the organic glass rod b. Activation of the hinged mechanism

Fig. 2 Schematic of “column” removal process with a pendulum hammer

Fig. 3 Global damage of FRAME2 (middle and right photos show damages of columns)

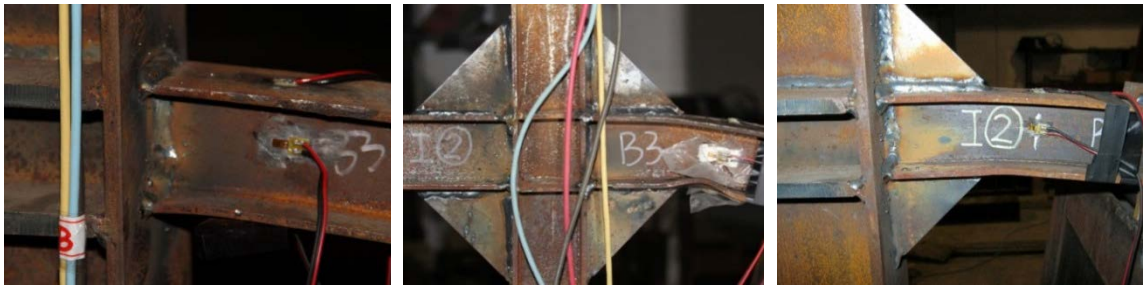

a. FRAME1 b. FRAME2 c. FRAME3

Fig. 4 Local buckling of beams near beam-to-column connection in the three test frames

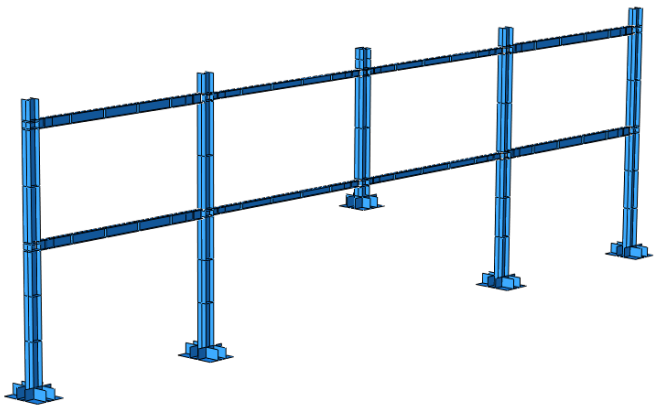

a. Overall frame configuration

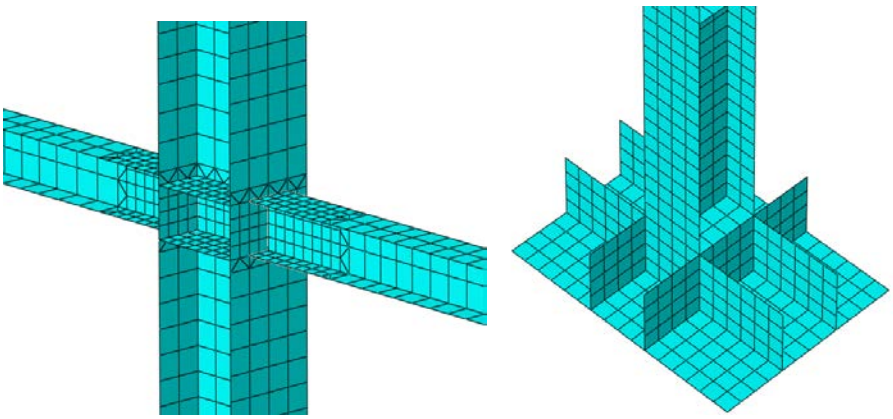

b. Detailed FE mesh

Fig.5 Finite element model of specimen FRAME1

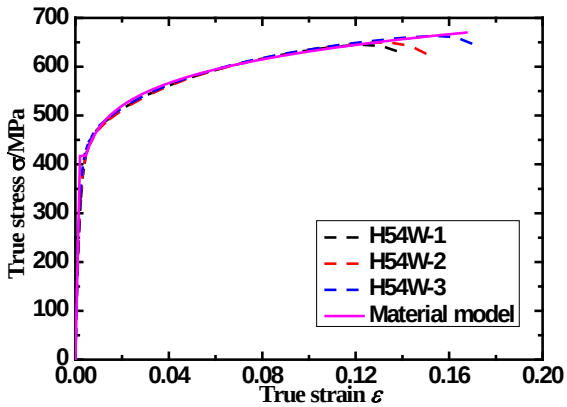

Fig.6 Comparison of true stress-strain curves from coupon tests with the theoretical model

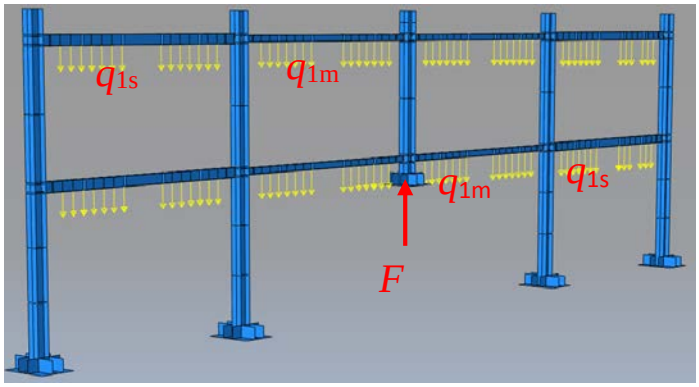

Fig.7 Reaction force F on the steel frame specimens

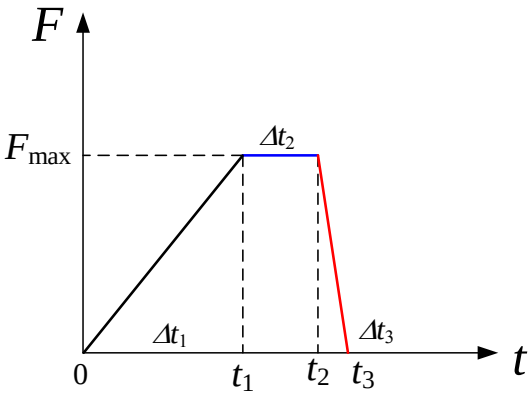

Fig. 8 Variation of reaction force

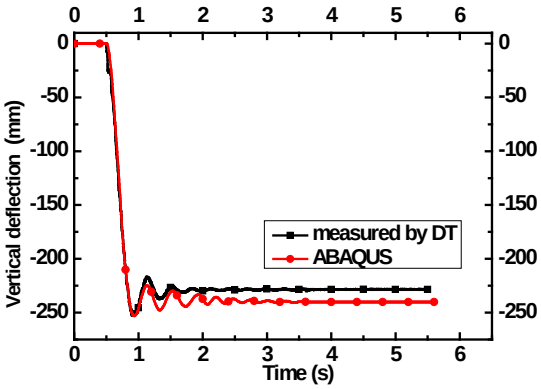

a. FRAME1

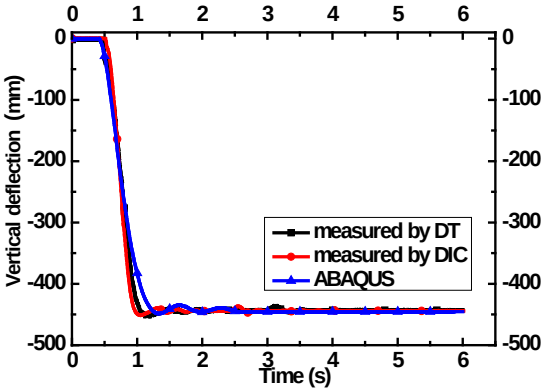

b. FRAME2

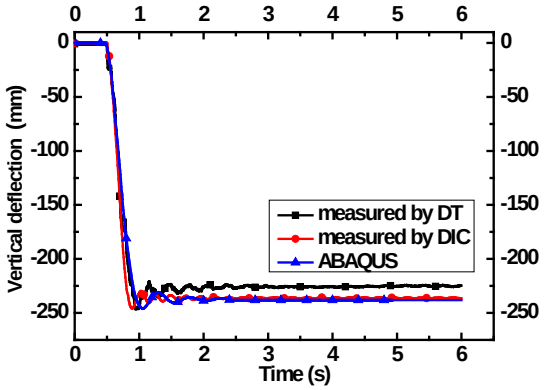

c. FRAME3

Note: DT = Displacement transducer

DIC = Digital Image Correlation

Fig.9 Comparison of the vertical deflection time histories with measurements and analysis

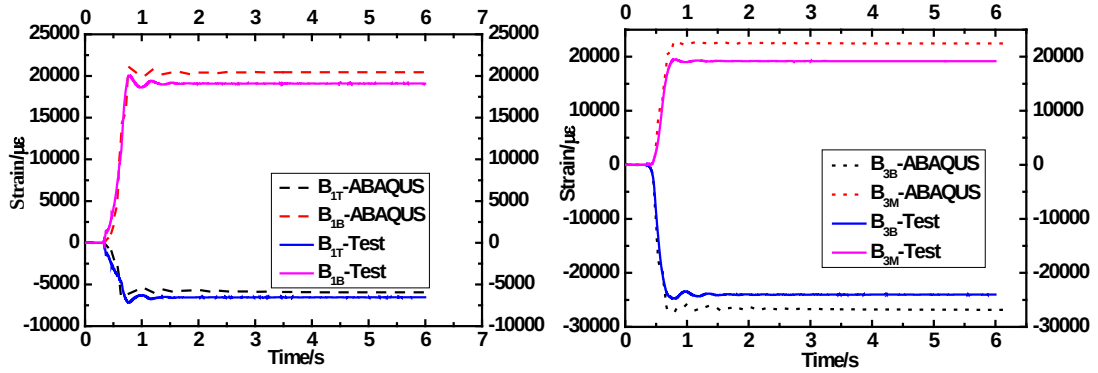

a. FRAME1

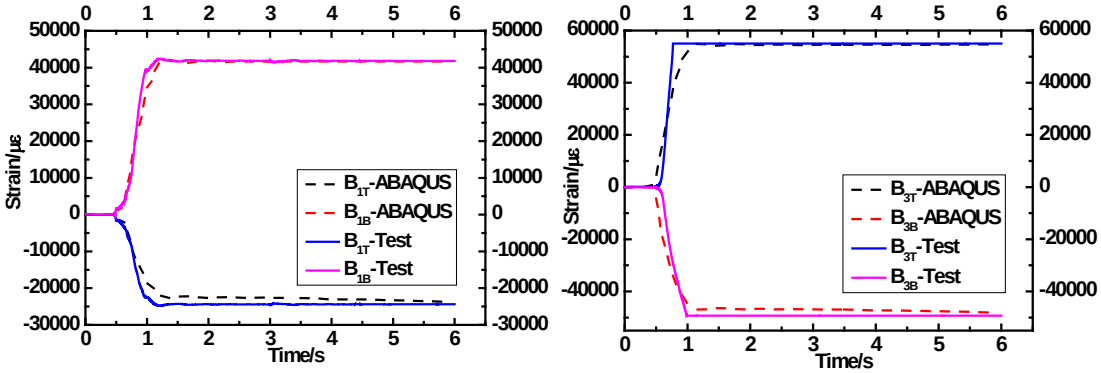

b. FRAME2

Fig. 10 Comparison of the strain time histories at beam sections B_1 and B_3

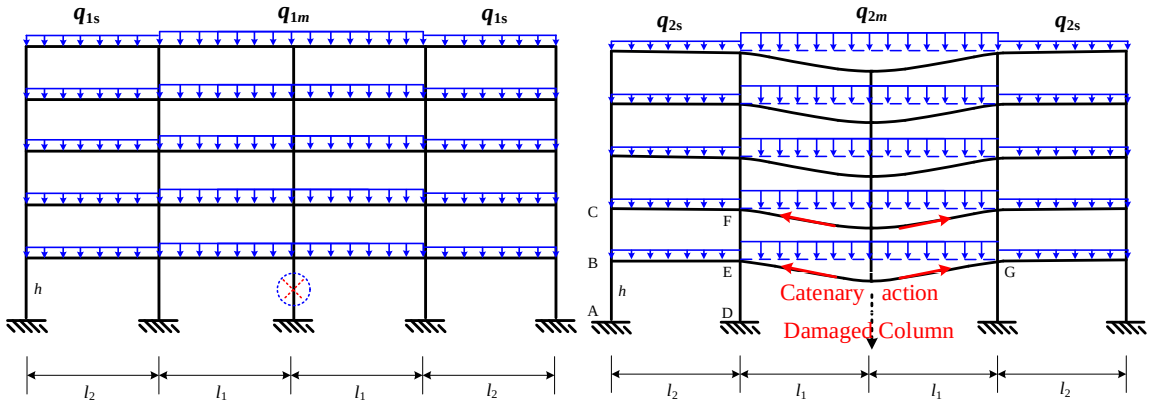

a. Intact structure b. Damaged structure

Fig. 11 Schematic of structural load

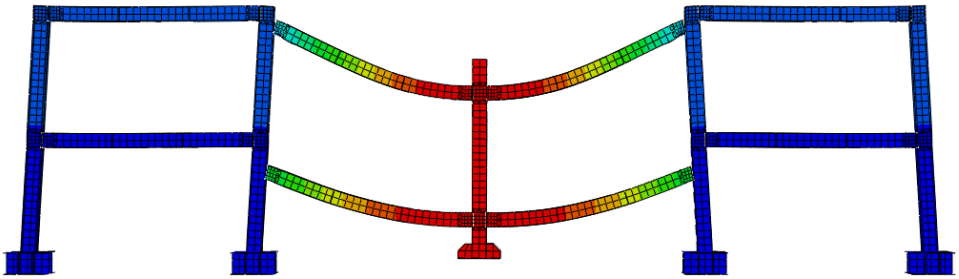

a. Contained progressive collapse mode (CCM)

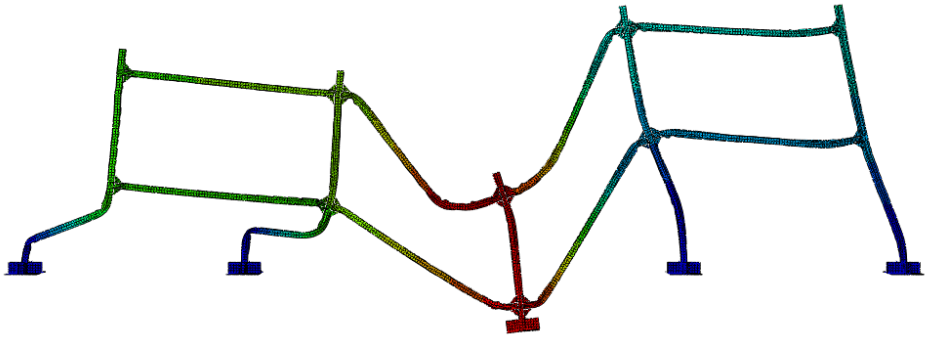

b. Propagating progressive collapse mode (PCM)

Fig. 12 Two representative progressive collapse modes of a steel frame as reproduced from FE analysis

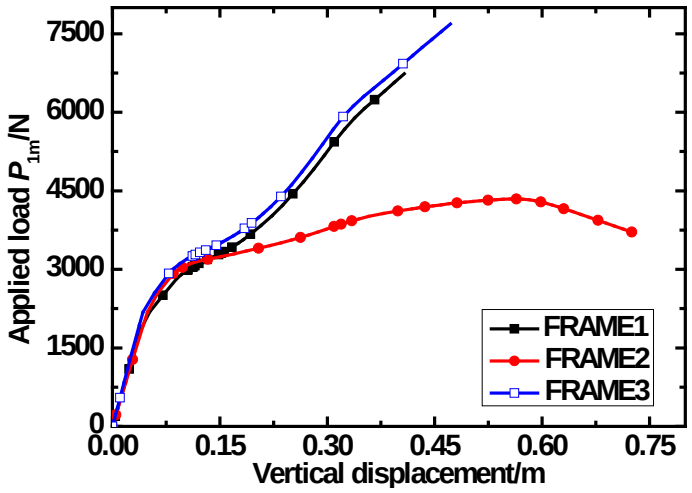

Fig.13 Static load-vertical displacement curves of the frame specimens with column removal

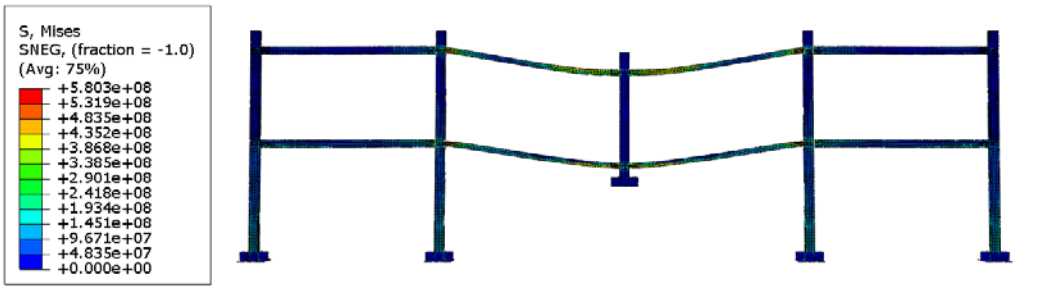

a. Dynamic analysis result

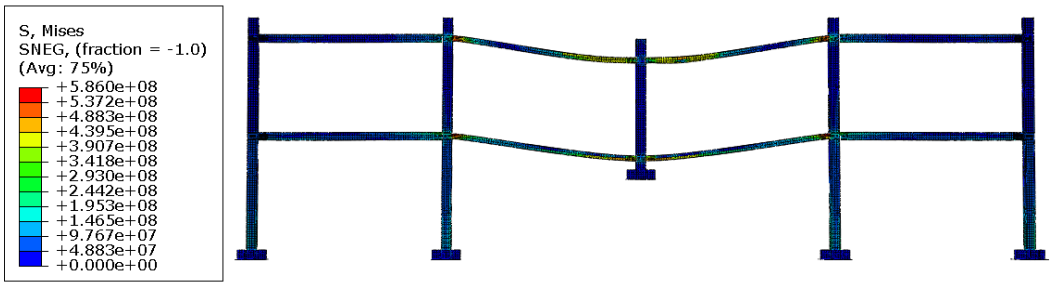

b. Static analysis result considering dynamic amplification factor

Fig.14 Comparison of deformations in FRAME1 after column removal between dynamic and equivalent static analyses

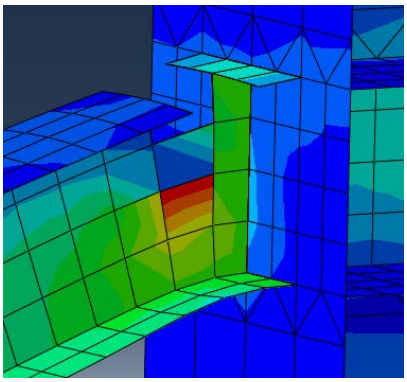

a. Fracture of first floor beam

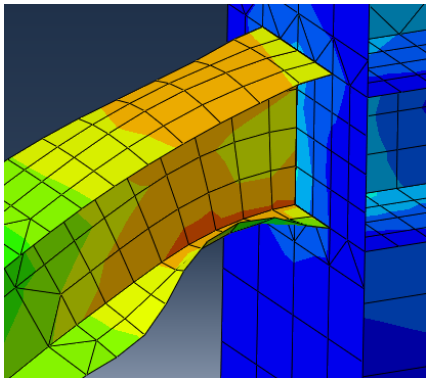

b. Buckling of second floor beam

Fig.15 Failure of beams near beam-to-column connections of FRAME1

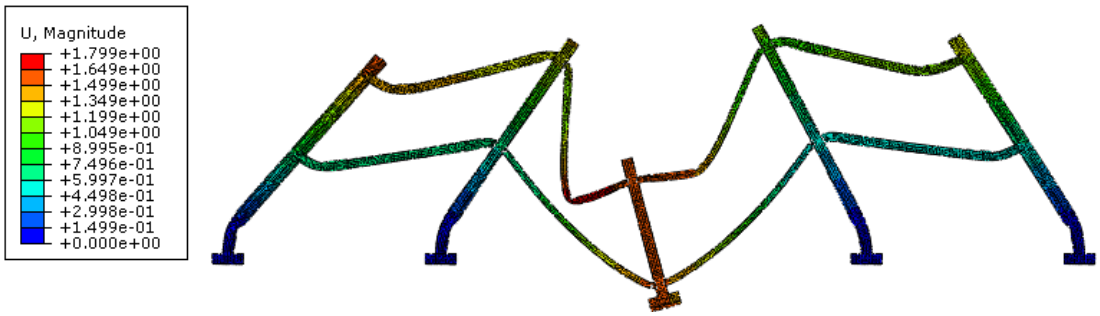

(a) FRAME1

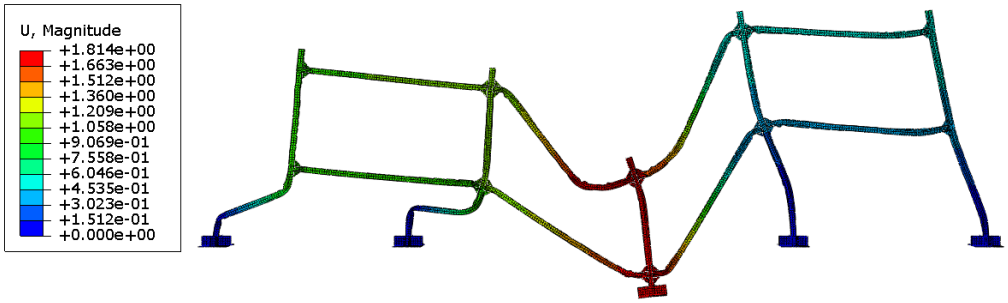

(b) FRAME2

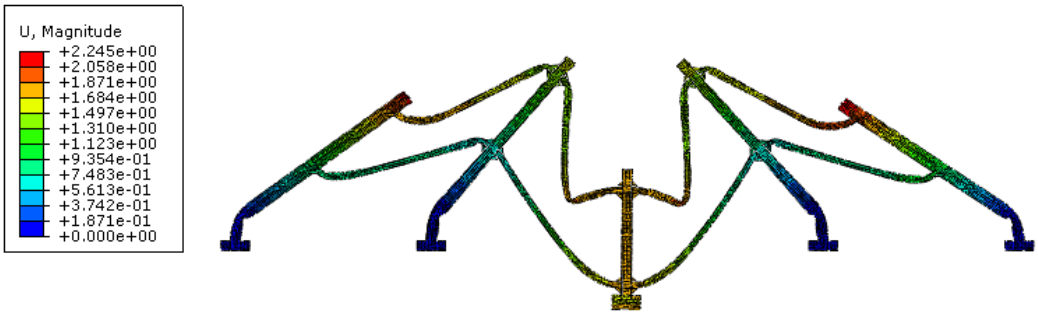

(c) FRAME 3

Fig.16 Collapse modes of the three steel frames

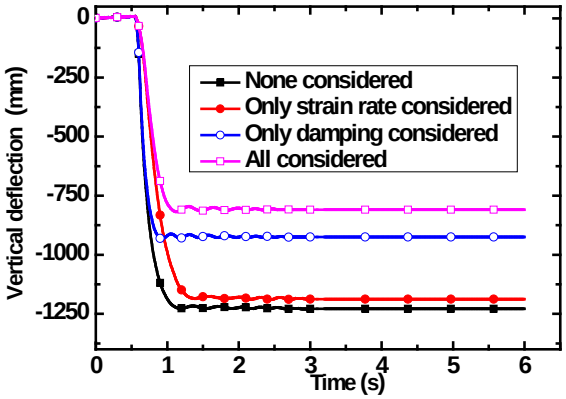

Fig. 17 Influences of strain rate effect and damping on the deflection time histories of FRAME1

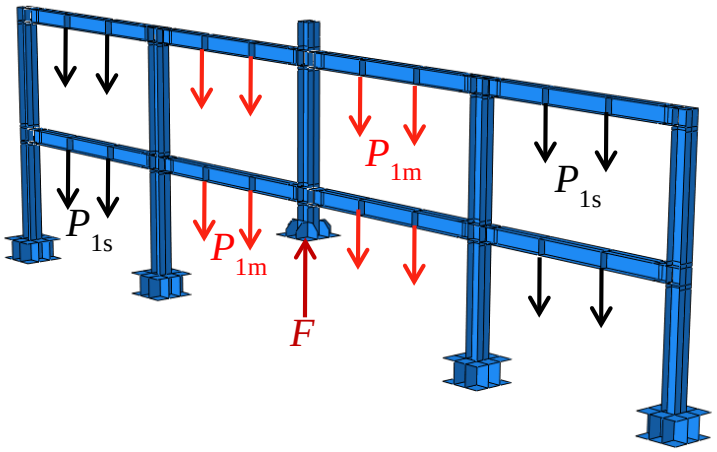

Fig. 18 Finite element model of FRAME4

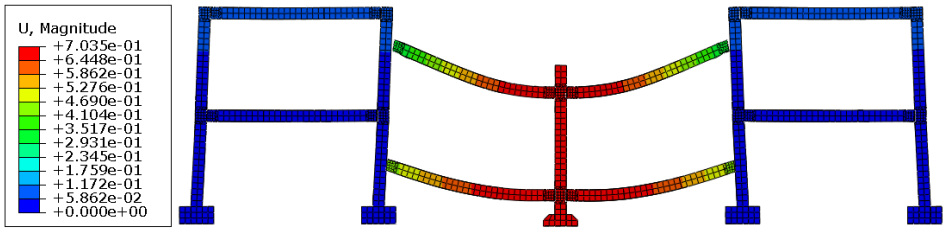

Fig.19 Collapse mode of FRAME4

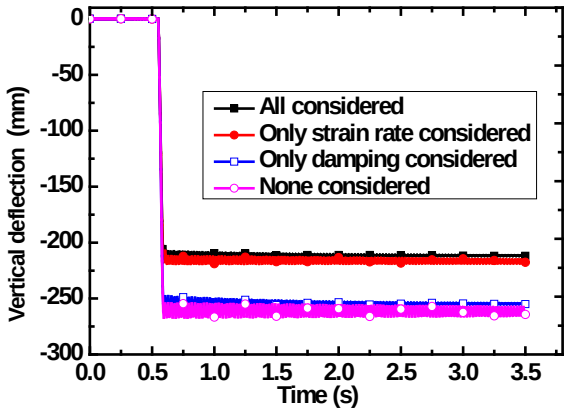

Fig. 20 Effects of strain rate and damping on the deflection time histories of FRAME4

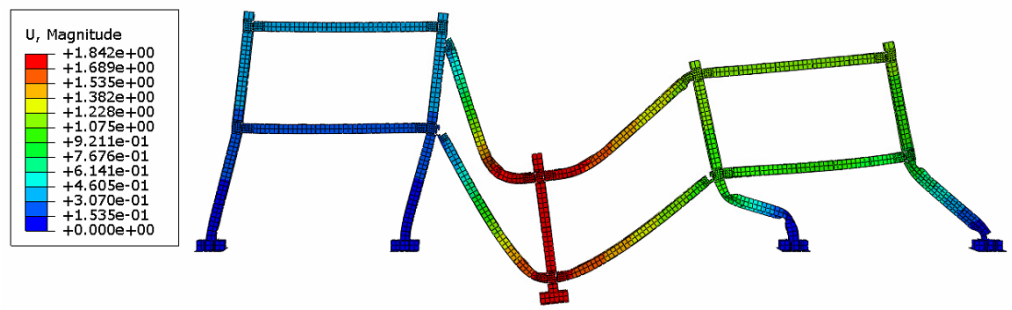

Fig. 21 Collapse mode of FRAME5

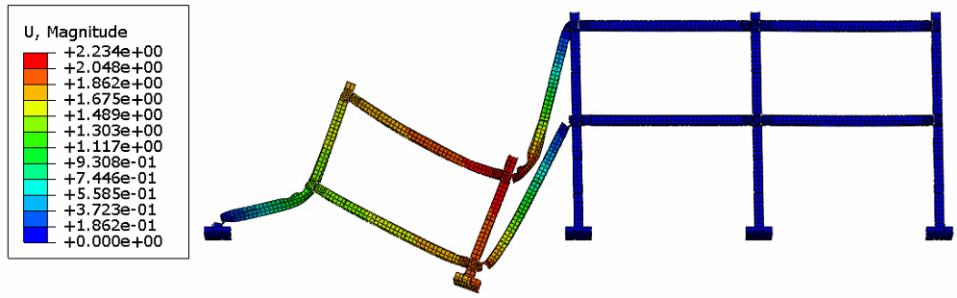

a. Collapse mode for a removed side-bay interior column

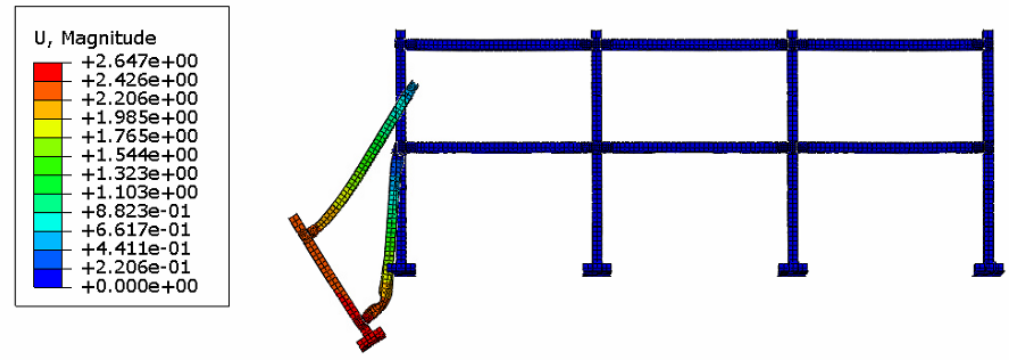

b. Collapse mode for a removed side column

Fig.22 Collapse modes corresponding to different locations of removed column